Maximum Power Point Tracking for Variable Speed Wind Turbines with DTC and DPC of MLCs Based on FLC

Prof. Dr. Ahmed Abd Elsattar
Prof .Dr. Ahmed M. Atallah
Elect. Power &Machine Dept., Faculty of Eng. Ain-Shames University, Cairo, Egypt
aasattar2@yahoo.com
Eng. El Sayed F. El Tantawy
Elect. Power& Machine Dept., Faculty Banha of Eng. Banha University, Qalubiya
elsayed_fraht@yahoo.com

Abstract. Multilevel converters are essential for high capacity turbines and medium voltage generation. This paper presents an optimum maximum power $P_{max}(W_{opt})$ technique to guaranty an optimal reference speed. PI controller and fuzzy logic controller for both direct torque control in machine side converter and direct power control of grid side converter with diode clamped five-level converter are implemented. The use of PI controller for both direct torque control and direct power control with multilevel converters is expected to decrease steady state error. It may increase peak overshoot and steady state time. And it cannot handle uncertainty (system parameters, sensor measurement). Replacing PI controller with fuzzy logic controller will decrease peak overshoot, steady state time and it can handle uncertainty. Direct torque control with fuzzy speed controller for multilevel converters improves the performance of wind turbine (MPPT) and Squirrel cage induction generator (speed, flux, torque and current) despite wind variation. Direct power control with fuzzy dc voltage controller for multilevel converters will improve power quality (the current injected to utility-grid). A comparison between PI controller and fuzzy logic controller for both machine side converter and grid side converter with diode clamped five-level converter has been done.

Key words: Direct Torque Control, Direct Power Control, Multilevel Converter, Maximum Power Point Tracking, Squirrel Cage Induction Generator, Fuzzy Logic Control.

1. Introduction

Energy is one of the most promising renewable energy sources. It has received tremendous progress at the recent year [1]. The trend in wind turbine systems has been towards large capacity units [2]. Using wind turbines with high capacity and variable the wind speed, it is preferred to use variable speed generators [3]. A Variable speed system, using Squirrel cage induction generator (SCIG) has to be connected to the utility-grid by bidirectional power flow back-to-back converter (AC-DC-AC converter). A variable speed wind turbine (VSWT) system has the advantages of reducing mechanical stresses, noise and fluctuations besides it produce high efficiency [4]. Moreover more energy is captured over a wide range of the wind speed variations. Thus variable speed systems are preferred to fixed speed [3, 4].

Medium voltage is usually with high power capacity wind turbine to reduce the generator current to acceptable level. This reduces cable cost, power losses and reduced stress, as well as improving the system power efficiency [4-8]. Power electronic converters play a crucial role in the integration of variable speed wind power system connected to the utility-grid [9]. When using medium voltage and high output power, multilevel converters (MLCs) are becoming the most promising candidates [4, 5]. Medium voltage power electronic converter like MLC topology has been gaining the popularity to eliminate the grid side step up transformers [8]. Diode clamped multilevel converter was used because it needs a Simple control algorithm and produce high efficiency [4]. The back-to back converters in Fig. 1 is consisting of two diodes clamped five-level back-to-back converters connected together via a DC link capacitor.

In a variable speeds system, a maximum power point tracking (MPPT) adjusts system quantity is to maximize wind turbine power output [3]. Efficiency of a variable speeds system is of great importance to harvest maximum power from incident wind [10]. To maximize wind turbine output energy, the MPPT control for variable speed system is indispensable when wind speed is below the rated speed. The MPPT, which aims to make the SCIG speed correspond to optimal value to ensure maximum energy production [11]. In order to extract maximum energy, the SCIG rotational speed has to be controlled accordingly by means of MSC (speed controller) [12]. There are many different MPPT such as optimum maximum power Pmax(wopt) curve, optimum TSR(tip speed ratio) control, power feedback control, hill climb searching control(perturb and observe & incremental conductance), and fuzzy-logic based control [3,13-15]. The optimum maximum power Pmax(wopt) curve, optimum TSR control requires

prior knowledge of wind turbine parameters to calculate the optimal operating point. These techniques are fast and simple [12]. The hill climb searching control, searches the maximum power with the use output power and rotational speed. These techniques need large time to reach MPPT during this time some amount of power loss takes place during the tracking phase [12].

The main function of MSC with SCIG is to optimize the energy captured from the wind by controlled generator speed with the reference speed given from the MPPT as will be shown in sec 3. Several control strategies of MSC to control SCIG have been developed [4], Such as, direct power control (DTC) [4, 16-24] and field oriented control (FOC) [10, 11, and 19, 25 - 30]. The FOC is complex, uses many SCIG parameters and constant gains of the PI controllers which cannot compensate wind speed variations [4, 19]. DTC uses less number of the SCIG parameters and sample. The Conventional DTC technique based on the use of PI controller with classical two-level converter has the drawbacks of having peak overshoot, steady state error, have low dynamic response. Besides SCIG parameters are variable and have same uncertainty of sensors measurement. So Conventional DTC with classical two-level converter has been replaced by MLC too solve the problem of peak overshoot, steady state error and low dynamic response [4, 24]. And PI controller has been replaced by fuzzy logic controller (FLC) to solve the problem of peak overshoot, and low dynamic response and uncertainty of SCIG parameters and measurement [16-18].

In [4] DTC with three and four MLC are used to solve the problem of Conventional DTC with classical two-level converter system faster , decrees steady stat error and decrees peak overshoot to some extent, but still peak overshoot high. Ref [22] used DTC space vector modulation with three multilevel in variable speed SCIG based wind energy conversion system. This technique has increase peak overshoot during the change of wind speed. In [16-18] uses DTC with two-level converter based on FLC is used to develop high performances of SCIG. But this technique increases the speed steady state error. Ref [24] Improve DTC of an SCIG used in a wind conversion system connected to the utility-grid. This algorithm based on a combination of DTC with the neural controller and the sliding mode technique. Also this algorithm increases the speed steady state error.

The main objective of grid side converter (GSC) with A VSWT system is to transfer and control the active power generated from wind generator to the utility-grid and control the DC bus voltage smoothly. Also it controls reactive power injected to the utility-grid and improvement Power quality of the injected power to the PCC (point of common coupling) decrease harmonics [23].

Reducing output current harmonics can be accomplished by: 1-increaseing the inductance of the filter, 2-increase the switching frequency and3-the use of MLC. Using high inductance in the filters causes an increase of the total cost and an increase of the device sizes. Moreover; the increase in the switching frequency results and of the total loss and overheating in power electronic switches [31]. The control strategies of GSC can be classified into two main categories: the first strategies based on a direct current Control such as VOC (voltage oriented control)[23, 26 and 30] and virtual flux oriented control. The second strategies based on the selection of an appropriate converter voltage vector such as direct power control (DPC) [23, 32-40] and virtual flux direct power control. The performances of VOC based on current control have low dynamic response, complex and increases THD for output voltage [23]. The performance of the DPC algorithm depends on accurate calculation of the active and reactive power. The advantages of Conventional DPC are: its Simplest, low THD in the current, its ability to produced high power factor (up to unity), good dynamic performance [23, 36].

The drawbacks of Conventional DPC technique based on PI controller (DC voltage controller) with classical two-level converter are the Poor THD in the output line voltage and its inability to treats uncertainties and variations of system parameter and sensor measurements [39]. The use of DPC with MLC is to improve THD of both output voltage and current. Using DPC with fuzzy (DC voltage controller) is to overcome the problems associated uncertainties of both system parameter and sensors measurement.

Ref. [39] uses a Predictive DPC for Three-Phase Grid-Connected Converters. In [36, 38] use MLC based on DPC to improve power quality. But this algorithm doesn't overcome uncertainties. In [32] A DPC strategy with proportional integrated regulator based wind power generation system is successively implementing the smooth active and reactive power output. But this system is complex because it uses an additional controller. Ref [34] uses Space Vector Modulation based on the DPC algorithm. This technique is a good choice for controlling the active and reactive power. But this technique produces high THD. In [37] uses DPC based on Sliding mode control to decrease THD and to the improve power factor. Ref. [20] uses a complex hybrid wavelet fuzzy neural network with VOC with the grid connected side. In [3] uses FLC and network controller to improve power quality. This techniques increase DC voltage steady state error.

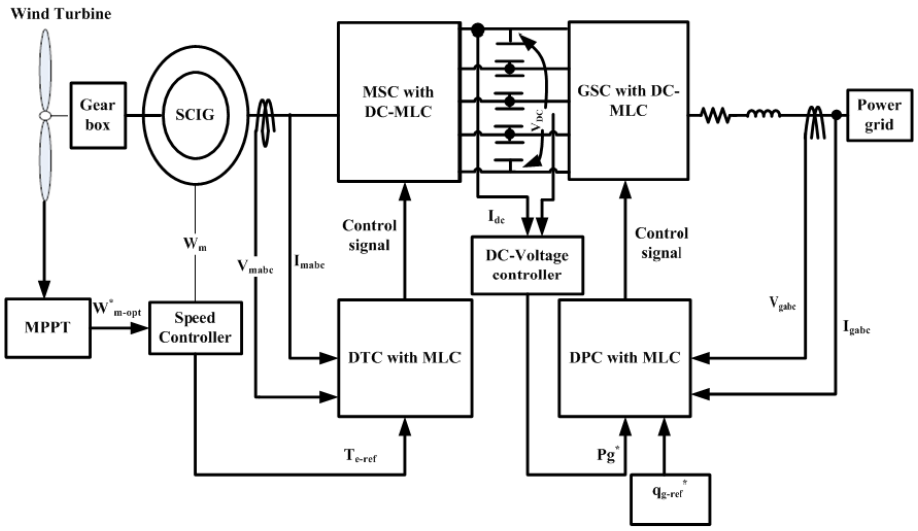

Figure 1: the proposed DTC and DPC schemes with MLC

In this paper, variable speed wind systems designed using SCIG connected with the utility-grid without transformer via a back-to-back diode clamped five level converters is presented in Fig. 1. MPPT algorithm has been introduced using The optimum $P_{max}(W_{opt})$ curve. It regulates the rotational speed to force the SCIG to work around its maximum power point in wind speeds below rated wind speeds. Also DTC with five level converters for MSC have been applied using both speed FLC and PI controller for compression. Moreover DPC with five-level converter for GSC have been applied using both DC voltage FLC and pi controller too. Comparisons between these techniques under wind speed changes are done to measure the performance due to the use FLC with five-level converter.

2. Wind turbine modeling

The mechanical power generated by VSWT at the turbine shaft as a function of power coefficients and TSR can be expressed as:

$$P_m = \frac{1}{2}\rho\pi R^2 v_w{}^3 C_P(\lambda,\beta) \quad (1)$$

$$\lambda = \frac{wR}{v_w} \quad (2)$$

$$C_P(\lambda,\beta) = C_1\left(\frac{C_2}{\lambda_i} - C_3\beta - C_4\right)e^{\frac{-C_5}{\lambda_i}} + C_6\lambda \quad (3)$$

$$\frac{1}{\lambda_i} = \frac{1}{\lambda + 0.08\beta} - \frac{0.035}{\beta^2 - 1} \quad (4)$$

Use the coefficients C1= 0.5176, C2= 116, C3=0.4, C4= 5, C5= 21, and C6= 0.0068. These coefficients depend on operating conditions of the wind turbine and the aerodynamic design of blade [3, 41]. Using the "NREL 5MW reference offshore wind turbine" model [4, 41].The peak power coefficient of CP= 0.482 at TSR of 7.55 and a fixed β=0. The mechanical turbine torque developed is given by:

$$T_m = \frac{P_m}{w_r} \quad (5)$$

The wind turbine shafts (Two mass drive train models) and the gearbox mechanical dynamic model are described as follows [41, 42].

$$T_m - T_L = J_r W_r + K_r W_r + B_r\theta_r \quad (6)$$

$$T_H - T_e = J_g W_g + K_g W_g + B_g\theta_g \quad (7)$$

$$G = \frac{W_g}{W_r} \quad (8)$$

3. Maximum Power Point Tracking Strategy

The control objective of MPPT is to captures the maximum of wind energy. In this work optimum maximum power $P_{max}(W_{opt})$curve technique is used. It uses a polynomial equation between optimum rotational speed and wind speed to produce the maximum power using wind tribune Properties.

Based on the equations (1-4), the actual mechanical power generated by turbine can be calculated as a function of rotational speed. Fig 2 presents the relation between mechanical powers versus rotational speed at deferent wind speed. For every wind speed exist single point for which the amount of mechanical power generated is the highest. The Blue dotted curve connecting these points. For maximum power generated the turbine should be operate at optimal rotational speed according this curve.

In this algorithm a fourth order polynomial equation is generated between optimal rotational speed and wind speed to guarantee a production of maximum power.

$$W_{opt} = -0.0003989\ V_w^4 + 0.01384\ V_w^3 - 0.1758\ V_w^2 + 11.43\ V_w - 1.938 \quad (9)$$

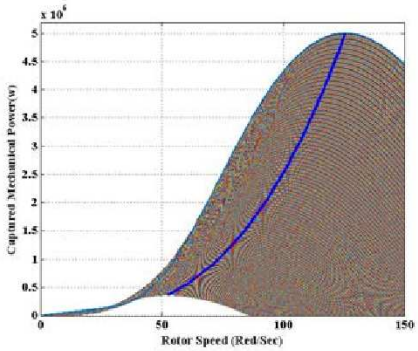

Figure 2: the mechanical power generated as a function of rotor speed of the turbine for variable speed wind

4. Diode clamped multilevel converter

Fig.1 shows the back-to-back five-level diode-clamped converters. Each converter (MSC, GSC) consists of number of power electronic switching equal (N-2)*2 and Diodes clamped required for each phase will be (N-1)*2. The MSC is connected between the SCIG and a capacitor bank. The GSC is connected between the capacitor bank and a second order filter connected to an electric grid. The numbers of capacitors used in diode clamped side are typically (N -1). The voltage across each capacitor is equal (Vdc/ (N-1)) [4, 36, 37].

The phase voltages with star connected for DC-MLC (MSC, GSC) model is expressed by the following equations (general equation):

$$V_{aN} = \frac{V_{DC}}{6(N-1)}\{2[S_{a1} + S_{a2} + \cdots + S_{a(n-1)} - S'_{a1} - S'_{a2} - \cdots S'_{Xa(n-1)}] - [S_{b1} + S_{b2} + \cdots + S_{b(n-1)} - S'_{b1} - S'_{b2} - \cdots S'_{b(n-1)}] - [S_{c1} + S_{c2} + \cdots + S_{c(n-1)} - S'_{c1} - S'_{c2} - \cdots S'_{c(n-1)}]\} \quad (10)$$

$$V_{bN} = \frac{V_{DC}}{6(N-1)}\{2[S_{b1} + S_{b2} + \cdots + S_{b(n-1)} - S'_{b1} - S'_{b2} - \cdots S'_{b(n-1)}] - [S_{a1} + S_{a2} + \cdots + S_{a(n-1)} - S'_{a1} - S'_{Xa2} - \cdots S'_{a(n-1)}] - [S_{c1} + S_{c2} + \cdots + S_{c(n-1)} - S'_{c1} - S'_{c2} - \cdots S'_{c(n-1)}]\} \quad (11)$$

$$V_{cN} = \frac{V_{DC}}{6(N-1)}\{2[S_{c1} + S_{c2} + \cdots + S_{c(n-1)} - S'_{c1} - S'_{c2} - \cdots S'_{c(n-1)}] - [S_{a1} + S_{a2} + \cdots + S_{a(n-1)} - S'_{a1} - S'_{a2} - \cdots S'_{a(n-1)}] - [S_{b1} + S_{b2} + \cdots + S_{b(n-1)} - S'_{b1} - S'_{b2} - \cdots S'_{b(n-1)}]\} \quad (12)$$

Fig.3 shows the five-level VSI space vectors voltage (SVV) in (α β) plane. The five levels converter has 125 possible states, 64 redundant switching states and 61 vectors (60 active vector and 0ne zero vector).

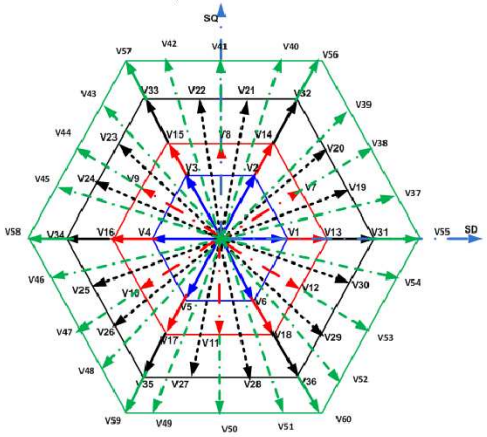

Figure 3: SVV of five-level converter

5. Squirrel Cage Induction Generator molding

The model of the SCIG, expressed rotor reference frame (d–q frame), is given by the following voltage system equations:

$$\left.\begin{aligned} V_{ds} &= R_s i_{ds} + \frac{d\phi_{ds}}{dt} - w_s\phi_{ds} \\ V_{qs} &= R_s i_{qs} + \frac{d\phi_{qs}}{dt} - w_s\phi_{qs} \\ 0 &= R_r i_{dr} + \frac{d\phi_{dr}}{dt} - w_r\phi_{dr} \\ 0 &= R_r i_{qr} + \frac{d\phi_{qr}}{dt} - w_r\phi_{qr} \end{aligned}\right\} \quad (13)$$

The flux equations are given by:

$$\left.\begin{aligned} \phi_{ds} &= l_s i_{ds} + m i_{dr} \\ \phi_{qs} &= l_s i_{qs} + m i_{qr} \\ \phi_{qs} &= l_r i_{dr} + m i_{ds} \\ \phi_{qr} &= l_r i_{qr} + m i_{qs} \end{aligned}\right\} \quad (14)$$

6. DTC with Five Levels Converter for Generator Side Converter

The control MSC with SCIG should be accurate and fast without any delay time. Also control the flux and torque of generator. The block diagram for DTC with five levels converter scheme is shown in Fig-4 which explains the control strategy [16].

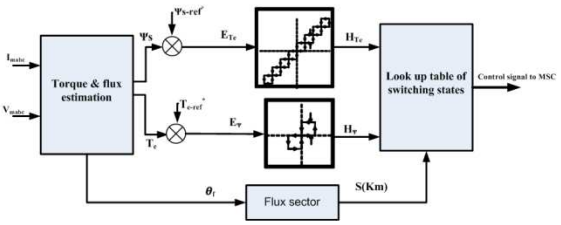

Figure 4: Block diagram of the DTC with five-level converter

In this algorithm, estimate the electromagnetic torque, magnitude and angle of stator flux of SCIG from these equations.

$$\psi_{s\alpha} = \int (V_{s\alpha} - R_s i_{s\alpha})\, dt \qquad (15)$$

$$\psi_{s\beta} = \int (V_{s\beta} - R_s i_{s\beta})\, dt \qquad (16)$$

$$|\psi_s| = \sqrt{\psi_{s\alpha}^2 + \psi_{s\beta}^2} \qquad (17)$$

$$\theta_{fs} = \mathrm{Tan}^{-1}\left(\frac{\psi_{s\beta}}{\psi_{s\alpha}}\right) \qquad (18)$$

$$T_e = \left(\frac{2}{3}\right)\left(\frac{P}{2}\right)\left(\psi_{s\beta} i_{s\alpha} - \psi_{s\alpha} i_{s\beta}\right) \qquad (19)$$

The stator flux magnitude estimated ψ_s is compared with reference (command) flux ψ^*_{s-ref}. The stator flux error E_ψ processed through three levels hysteresis band controller as shown in Fig-4. The estimated electromagnetic torque of SCIG T_e compare with reference torque T^*_{e-ref} computed from the speed controller. The electromagnetic torque error E_{Te} processed during nine levels hysteresis band controller.

HTe = 4 for $E_{Te} > 4HBT$
HTe= -4 for $E_{Te} < -4HBT$
HTe = 3 for $3HB < E_{Te} < 4HBT$
HTe= -3 for $-4HB < E_{Te} < -3HBT$
HTe= 2 for $2HBT < E_{Te} < 3HBT$
HTe= -2 for $3HBT < E_{Te} < -2HBT$
HTe= 1 for $HBT < E_{Te} < 2HBT$
HTe= -1 for $-2HBT < E_{Te} < -HBT$
HTe= 0 for $-HBT < E_{Te} < HBT$

The sector angel S(KM) calculated from the angle of the stator flux θ_{fs} . Total sectors number is 24 sectors. Through output of stator flux hysteresis $H_{\psi s}$, electromagnetic torque H_{Te} hysteresis controllers and flux sector number are used to select the optimal SVV from optimal look up table. Voltage vector look up table for five levels converter is from sector (S1) to sector (S12) is given in Table 1.

7. Speed Controller Designed

7.1. Design of PI Controller

The conventional PI Controller is simple controller. This controller is described by the following equation

$$U(t) = K_p e(t) + K_i \int e(t) dt \qquad (20)$$

The gains (kp.ki) are adjusted by trial and error process such that the system gives a good performance.

7.2. Design of Fuzzy logic Controller

In FLC, the basic of control action is determined by a set of linguistic rules. These linguistic rules are determined by the system. The numerical variables are converted into linguistic variables. Mathematical system modeling is not required in FLC. The FLC comprises of three parts: fuzzification, interference and defuzzification.

The basic structure of FLC with speed is given in fig-5, where the two inputs to the FLC are the normalized values of speed error 'Ew' and rat of change of speed error 'dEw'. The output torque reference Te^* of the FLC1 is then multiplied with a gain 'KT' to demoralize the output torque value. The membership functions sets of speed error, rat of change of speed error and the corresponding output torque are given in fig 6.

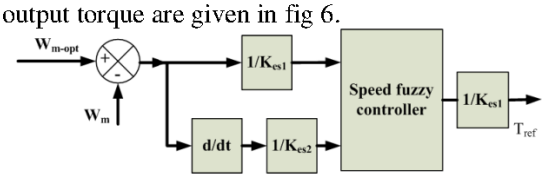

Figure 5: Block diagram of the FLC with generator speed

The input and output membership functions are chosen by a trial and error basis such that the controller gives optimum results. The rule base for the speed fuzzy controller is given in table-2.

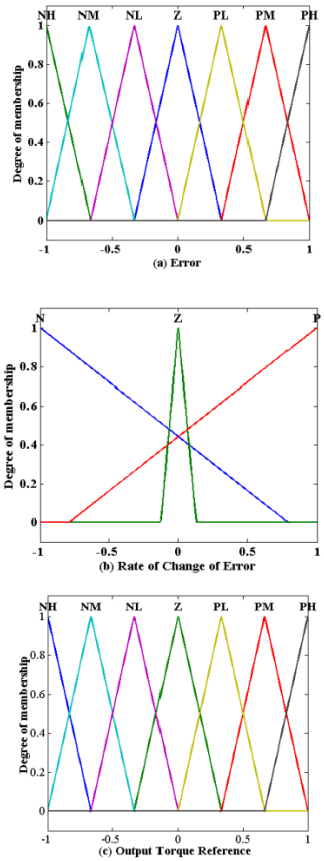

Figure 6: Membership functions: (a) error input to speed FLC, (b) rate of error change input to speed FLC, (c) output of speed FLC

Table 1: Optimum selections voltage vector look up table for DTC with five-level converter from sector (S1) to sector (S12).

H_ψ	H_T	θ_1	θ_2	θ_3	θ_4	θ_5	θ_6	θ_7	θ_8	θ_9	θ_{10}	θ_{11}	θ_{12}
1	4	V56	V56	V57	V57	V57	V57	V58	V58	V58	V58	V59	V59
1	3	V37	V38	V38	V39	V40	V41	V41	V42	V43	V44	V44	V45
1	2	V19	V20	V20	V32	V21	V22	V22	V33	V23	V24	V24	V34
1	1	V7	V7	V2	V14	V8	V8	V3	V15	V9	V9	V4	V16
1	0	V0	V0	V0	V0	V0	V0	V0	V0	V0	V0	V0	V0
1	-1	V18	V6	V12	V12	V13	V1	V7	V7	V14	V2	V8	V8
1	-2	V36	V29	V30	V30	V31	V19	V20	V20	V32	V21	V22	V22
1	-3	V52	V53	V53	V54	V37	V38	V38	V39	V40	V41	V41	V42
1	-4	V60	V60	V55	V55	V55	V55	V56	V56	V56	V56	V57	V57
0	4	V19	V20	V20	V21	V22	V22	V23	V23	V24	V24	V24	V25
0	3	V7	V7	V8	V8	V8	V8	V9	V9	V9	V9	V10	V10
0	2	V14	V14	V15	V15	V15	V15	V16	V16	V16	V16	V17	V17
0	1	V2	V2	V3	V3	V3	V3	V4	V4	V4	V4	V5	V5
0	0	V0	V0	V0	V0	V0	V0	V0	V0	V0	V0	V0	V0
0	-1	V6	V6	V1	V1	V1	V1	V2	V2	V2	V2	V3	V3
0	-2	V17	V17	V18	V18	V18	V18	V13	V13	V13	V13	V14	V14
0	-3	V11	V11	V12	V12	V12	V12	V7	V7	V7	V7	V8	V8
0	-4	V27	V28	V28	V29	V29	V30	V30	V19	V19	V20	V20	V21
-1	4	V57	V57	V58	V58	V58	V58	V59	V59	V59	V59	V60	V60
-1	3	V41	V41	V42	V43	V44	V44	V45	V46	V47	V47	V48	V49
-1	2	V33	V23	V24	V24	V34	V25	V26	V26	V35	V27	V28	V28
-1	1	V15	V3	V9	V9	V16	V4	V10	V10	V17	V5	V11	V11
-1	0	V0	V0	V0	V0	V0	V0	V0	V0	V0	V0	V0	V0
-1	-1	V18	V6	V12	V12	V13	V1	V7	V7	V14	V2	V8	V8
-1	-2	V36	V29	V30	V30	V31	V19	V20	V20	V32	V21	V22	V22
-1	-3	V52	V53	V54	V54	V37	V38	V39	V39	V40	V41	V42	V42
-1	-4	V55	V55	V56	V56	V56	V56	V57	V57	V57	V57	V58	V58

Table 2: Rule base for speed FLC

		rate of change error change						
		NP	NM	NS	Z	PS	PM	PL
Error	N	NP	NM	NM	NS	PS	PS	PM
	Z	NP	NM	NS	Z	PS	PM	PL
	P	NM	NS	NS	PS	PM	PM	PL

8. DPC with Five-Level Converter

The objective of the grid side five-level converter is to controls active power transfer to the utility-grid, reactive power to zero in order to fix the unity power factor and regulate the dc-link voltage. The control system of DPC with MLC is presented in Fig. 7.

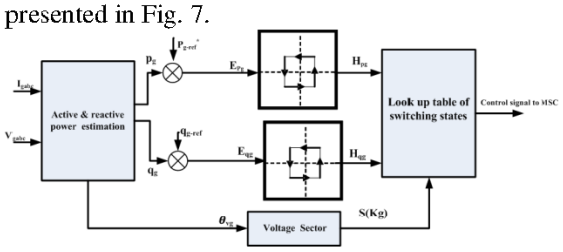

Figure 7: Block diagram of the DTC with five-level converter

In this technique, measured line voltages and currents (Vgabc ,igabc) at PCC of the grid. This measured signals (Vgabc , igabc) converted to rotating reference frame (d,q).

From v_{gd}, v_{gq}, i_{gd} and i_{gq} active and reactive power of the grid is calculated using following Equations.

$$P_g = \frac{3}{2}\left(v_{gd}i_{gd} + v_{gq}i_{gq}\right) \qquad (21)$$

$$q_g = \frac{3}{2}\left(v_{gq}i_{gd} - v_{gd}i_{gq}\right) \qquad (22)$$

The calculated active power Pg is compared with reference active power Pref computed from DC voltage controller as shown in fig 8.The error in active power EP processed through two levels hysteresis controller.

Also the reactive power qg calculated compared with reference reactive power qgref (qgref set to zero for unity power factor in this paper). The reactive power error pressed through two level band hysteresis controllers.

The sector number of grid is calculated from grid voltage angle, Eq 23. The total number of sectors is 24 sectors.

$$\theta_g = \mathrm{Tan}^{-1}\left(\frac{v_{gq}}{v_{gd}}\right) \qquad (23)$$

Through output of active, reactive controllers and voltage sector the optimal SVV is selected in each sampling interval. Table.3 illustrates the proposed DPC system for five levels converter to be selected for optimal SVV from sector 1 to sector 12.

Table 3: Optimum selections voltage vector look up table for DPC with five-level converter from sector (S1) to sector (S12).

H_p	H_q	θ_1	θ_2	θ_3	θ_4	θ_5	θ_6	θ_7	θ_8	θ_9	θ_{10}	θ_{11}	θ_{12}
1	1	V1	V7	V8	V9	V2	V10	V11	V12	V3	V13	V14	V15
1	-1	V9	V2	V10	V11	V12	V3	V13	V14	V15	V4	V16	V17
-1	-1	V48	V25	V33	V56	V43	V26	V35	V57	V44	V27	V37	V58
-1	0	V35	V57	V44	V27	V37	V58	V45	V28	V39	V59	V46	V29

9. DC voltage controller

The reference active power is deduced by controlling the direct bus voltage with the DC voltage controller generating the current reference ic−ref to the capacity

Hence, we can express Pref as:

$$P_{\text{ref}} = V_{dc}(i_{dc} - i_{cref}) \quad (24)$$

$$P_{\text{ref}} = P_{dc} - p_{\text{cref}} \quad (25)$$

$$i_{cref} = ouput\ of\ \text{DC voltage controller}(V_{dc-ref} - V_{dc}) \quad (26)$$

Fig. 8 shows a block diagram DC voltage controller. For maintaining a constant voltage with PI or FLCs generating the reference current in the capacitors

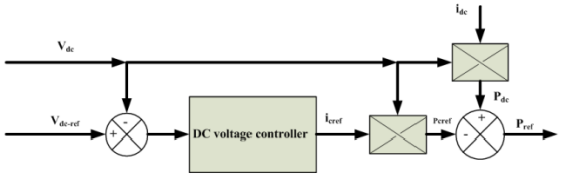

Figure 8: Block diagram of the DC voltage controller

9.1. DC voltage controller designed

The control of the DC link voltage consists of ensuring that all the active power produced by the SCIG is transferred to the utility grid [7].The DC voltage controller designed with PI controller by equation (20). Fig 9 presents the structure of the DC voltage controllers for five level converters with mamdani-type fuzzy controller. In the design of DC voltage controller using FLC, two variables inputs is used 1- DC voltage error 'Edc' and 2- the rat of change of DC voltage error 'dEdc'. The output is the reference current in the capacitors icp-ref.

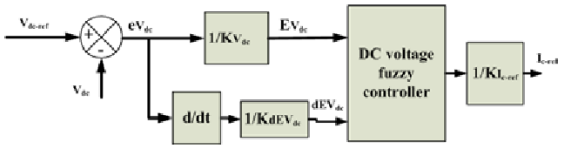

Figure 9: Block diagram of the FLC with DC voltage

Membership functions are assigned to the linguistic variables, using seven Triangular fuzzy subsets shown in Fig. 10 for the input and output. Table 4 displays the rules governing the controller's operation.

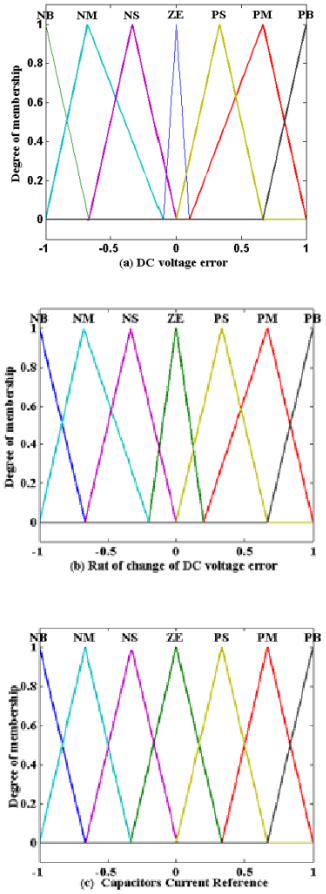

Figure 10: Membership functions: (a) error input to DC voltage FLC, (b) rate of error change input to DC voltage FLC, (c) output of DC voltage FLC(capacitors reference current)

Table 4: Rule base for DC voltage FLC

		Rat of change of DC voltage error						
		NB	**NM**	**NS**	**ZE**	**PS**	**PM**	**PB**
DC voltage error	**NB**	NB	NB	NB	NB	NM	NS	ZE
	NM	NB	NB	NB	NM	NS	ZE	PS
	NS	NB	NB	NM	NS	ZE	PS	PM
	ZE	NB	NM	NS	ZE	PS	PM	PB
	PS	NM	NS	ZE	PS	PM	PB	PB
	PM	NS	ZE	PS	PM	PB	PB	PB
	PB	ZE	PS	PM	PB	PB	PB	PB

10. Simulation and Result Analysis

The complete system Mathematical model and simulation are implemented under Matlab /Simulink SimPowerSystems, using wind speed variations, Fig.11. Forcing reference reactive power to zero guarantee unity power factor during different wind speeds. The simulation results are divided into two cases depending on both speed and DC voltage controllers. Case (a) is composed

of DTC with PI speed controller for machine side five-level converter and DPC with PI DC voltage controller for grid side five-level converter. Case (b) is composed of DTC with fuzzy speed controller for machine side five-level converter and DPC with fuzzy DC voltage controller for grid side five-level converter. Wind turbine characteristics "NREL 5MW wind turbine" and the parameters of SCIG are listed in Appendix A and [4].

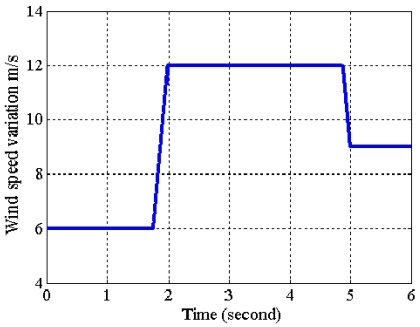

Figure 11: Wind speed variations

Fig. 12 shows the performance of the dynamic responses between reference speeds calculated from MPPT algorithm and actual speed of SCIG. From this Figure the steady state time is decreased with FLC in this work and takes lesser time and Refs [4, 13]. Also the starting speed is decreased (table 5).

Following the output of the proposed MPPT (taken as reference speed) using a) PI controller and b) FLC we have got the results given in Fig. 12.

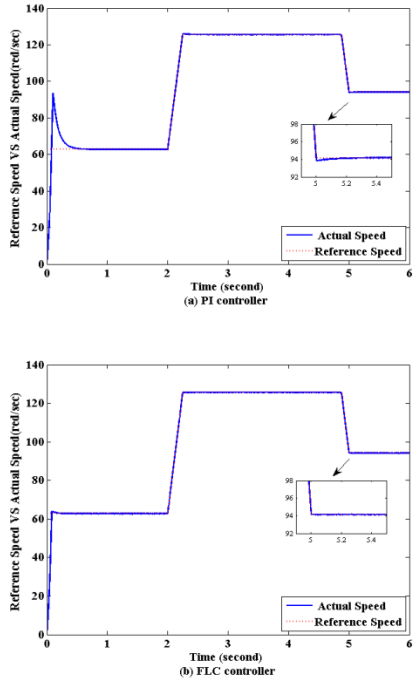

Figure 12: the SCIG reference& actual speed (a) PI controller and (b) FLC controller.

Fig. 13 shows the speed error between reference and actual speeds decreases for with FLC. This leads to higher efficiency of a VSWT system. Moreover, Refs [4, 13,14,17,21, 22and 28] gives a speed error much higher than that in the proposed system with FLC (table 5).

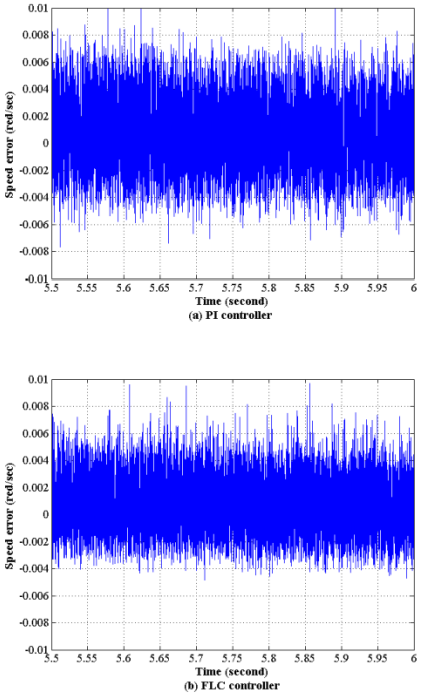

Figure 13: the speed error (a) PI controller and (b) FLC controller.

Fig 14 shows the electromagnetic torque of induction generator which is depend on wind speed variations in Fig 11. The peak overshoots decrease with FLC at start-up and wind speed changes at 4.8 Sec.

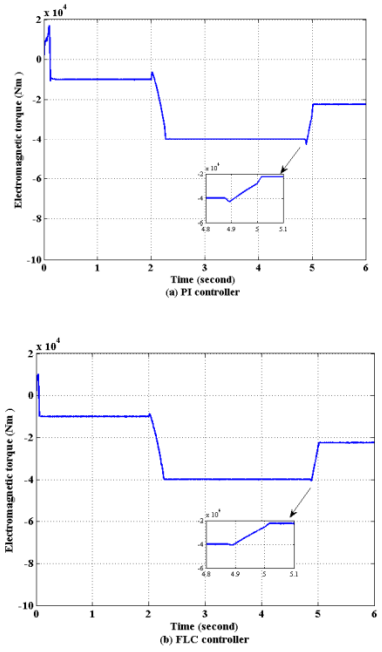

Figure 14: the electromagnetic torque of SCIG a) PI controller. (b) FLC controller.

Fig. 15 gives the locus diagram of the stator flux components in stationary reference frame (α β). The stator flux is less distortion with FLC and makes an ideal circular shape. The FLC with MLC technique gives better results than Refs [4, 13 and16].

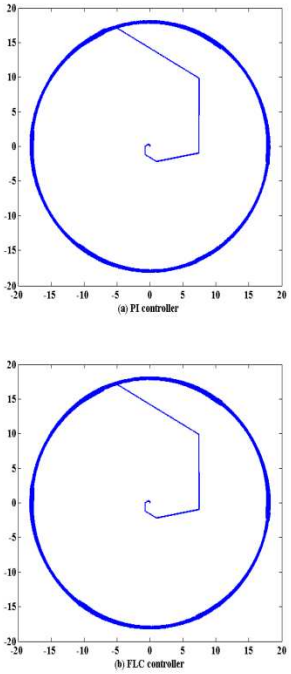

Figure 15: The stator flux in (α β) frame. a) PI controller (b) FLC controller

Fig. 16 depicts the performance of responses between the references and actual the DC link voltages. From this Fig., peaks overshoot decreases during the starting with FLC, besides the steady state time decrees with FLC. From this fig. the DC bus voltage almost constant with the change in wind speeds. The DC bus voltage ripples are reduced using FLC (table 5) and steady state time needed to reach the steady state and the dc link voltage ripples in this work is less compared with Ref[3,5, 16 ,17 and 19].

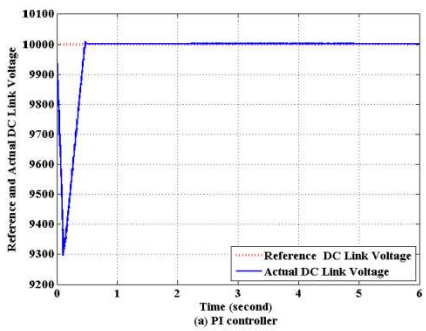

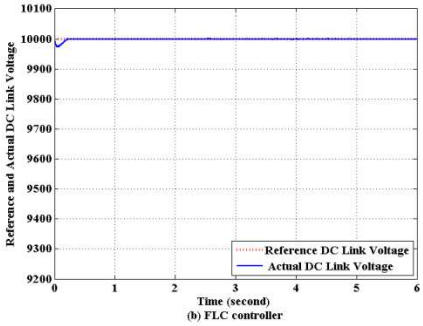

Figure 16: the reference and actual DC link voltage (a) PI controller (b) FLC controller

Fig.17 shows the grid injected current at PCC. The FLC decreases transient current (table 5). The proposed controller system (FLC) gives current with lesser distortion which improves the power quality.

Fig 18 shows the THD for three-phase current injected to the utility-grid at rated wind speed. THD decreases with FLC and improve power quality (table 5). It's lower than the 5% limit mandatory by IEEE- 519 standard and much better than the output results of Refs [13, 18and 19].

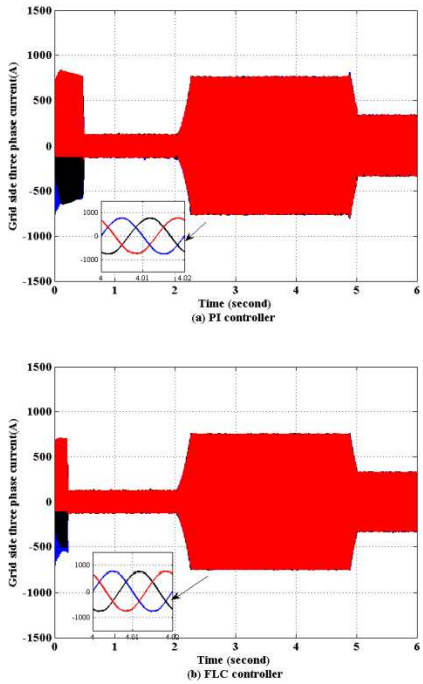

Figure 17 : Three-phase utility-grid current. (a) PI controller. (b) FLC controller

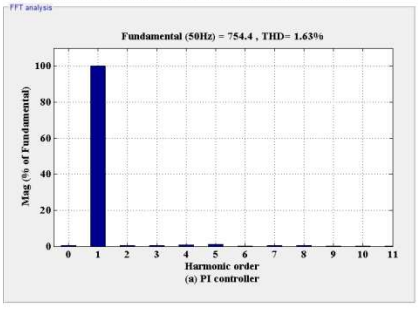

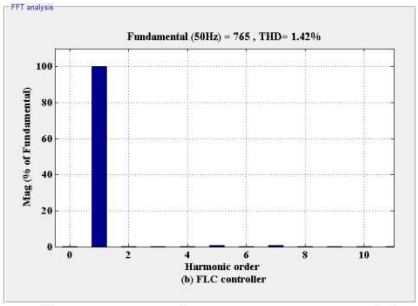

Figure 18: the THD of the three-phase utility-grid current (a) PI controller (b) FLC controller

Fig 19 presents the performances of power factor for the power injected to the utility-grid. The power factor of power injected to the utility-grid almost constant at unity power factor.

Figure 20 shows the active power transfer to the utility-grid. The peak overshoots of active power decrease with FLC at wind speed variation at 4.8 Sec.

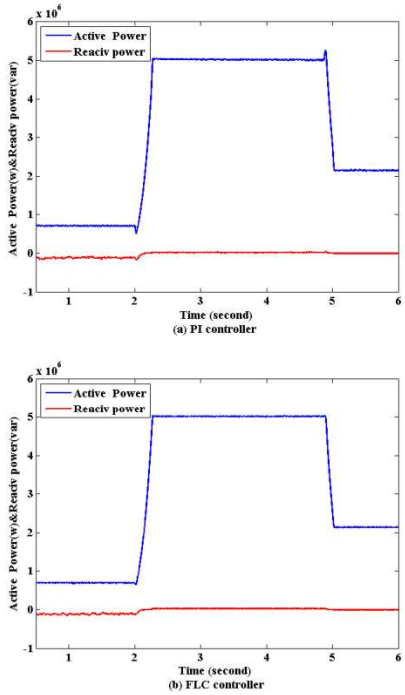

Figure 19: Active Power of the utility-grid (a) PI controller (b) FLC controller.

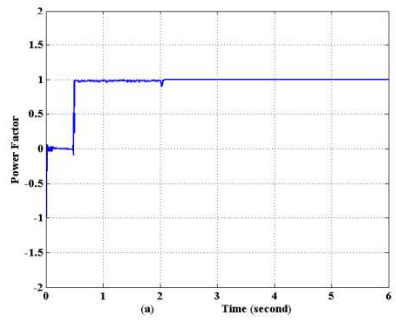

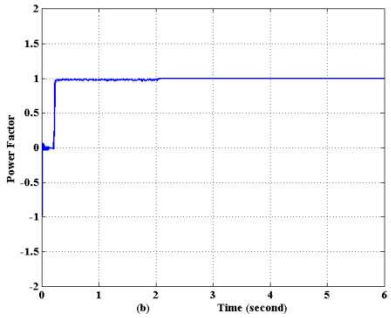

Figure 20: the utility-grid power factor. (a) PI controller (b) FLC controller

Table 5 collects the performance of PI and FLC with five-level converter for comparisons. Finally, the FLC with five-level converter give better performance with decrees starting speed, error, THD, and settling time.

Table 5: Comparison between the proposed schemes

	PI with 5-L Converter	FLC with 5-L Converter
steady state time	0.5 Sec	0.2 Sec
Starting speed	48%	1.5%
Speed error range	0.0013%	0.0012%
DC voltage ripple	5 V	1 V
THD OF current	1.63%	1.42%
Starting current	high	Low

11. Conclusion

A polynomial to represent MPPT is implemented with FLC to maximize captured power of wind turbine. Also the design of DTC with conventional PI speed controller as well as FLC for generator side diode clamped five-level converter is used. Besides; the grid side diode clamped five-level converter with DPC for both PI and FLC of DC voltage controller is done too. A comparison between the performance of conventional PI controller and FLC with five-level converter are depicted and collected in Table 5. The results show that the performance of wind turbine and SCIG has been improved for the case of using 1) - the polynomial with MPPT 2)-FLC 3) –DTC and DPC with five-level converter. The improvements (Figures 12-20) such that 1-Steady stat speed error have been decreased (increase efficiency), 2-steady stat time is decreased (fast

dynamic response),3- peak overshoot has decreased, 4- transient responses with wind speed variation has been improved.5- Decreases ripple of DC link voltage, 6-decreases THD in current injected to the utility-grid and 7- improves the power factor of the injected power to the utility-grid (unity power factor).All simulation models use the Simulink and Sim PowerS ystems for the NREL 5 MW wind turbines.

Appendix [A] the used grid parameters

Parameter	Value	Unit
Dc-bus voltage	**10000**	**V**
Dc-bus capacitor	**1500**	**uF**
Grid Filter resistance	**0.151**	**Ω**
Grid Filter inductance	**1.2**	**mH**
line to line voltage	**6600**	**V**
Frequency	**50**	**HZ**

Symbols and abbreviations

FLC	Fuzzy Logic Controller
PCC	Point Of Common Coupling
TSR	Tip Speed Ratio
MLC	Multilevel Converter
DTC	Direct Torque Controller
THD	Total Harmonic Distortion
SCIG	Squirrel Cage Induction Generator
DPC	Direct Power Control
DFIG	Doubly-Fed Induction Generator
MSC	Machine Side Converter
DC-MLC	Diode Clamped Multilevel Converter
FOC	Field Oriented Control
GSC	Grid Side Converter
VOC	Voltage Oriented Control
PI	Proportional Integral
N	Number Of Converter Levels
MPPT	Maximum Power Point Tracking
wr	Rotor Speed
Rs	Stator Resistance
Rr	Rotor Resistance
HBP	Power Hysteresis Band Width
HBT	Torque Hysteresis Band Width
Θsf	Stator Flux Angle
Θg	The Grid Position Angle
VSWT	Variable Speed Wind Turbine
Wm-opt	Speed Command (Reference)
Te-ref	Reference Electromagnetic Torques
HT	Output Of Hysteresis Controller
V_w	Wind Speed At The Centre Of The Rotor
Wr	Rotor Speed
Pm	Mechanical Power Extracted From The Wind
ρ	Air Density
C_p	Performance Coefficient
Vw	Wind Speed
A	Swept Area Of Rotor
B	Blade Pitch Angle
Λ	Tip Speed Ratio
Jr	Rotor Moment Of Inertia
Jg	Generator Moment Of Inertia
Kr	Rotor Coefficient Of Viscous Reaction
Kg	Generator Of Viscous Reaction
Br	Rotor Stiffness
Bg	Generator Stiffness
Tm	Shaft Torque At Wind Turbine
TL	Generator Torque Before Gear Box
TH	Generator Torque After Gear Box
Te	Generator Torque
G	Gear Speed Ratio
wg	Generator Speed
SVV	Space Voltage Vector

References

[1] Yaxing Renand , Liuying Li , Joseph Brindley and Lin Jiang," Nonlinear PI control for variable pitch wind turbine", Science Direct, Elsevier Control Engineering Practice, Vol. 50, PP 84-94 7 February 2016.

[2] Suman Debnath and Maryam Saeedifard," A New Hybrid Modular Multilevel Converter for Grid Connection of Large Wind Turbines" IEEE Transactions on Sustainable Energy, Vol. 4, PP. 1051–064, October 2013.

[3]Ahmed Medjber, Abderrezak Guessoum, HocineBelmili and Adel Mellit,"New neural network and fuzzy logic controllers to monitor maximum power for wind energy conversion system", Science Direct, Elsevier Energy, Vol. 106, PP 137-146, 6 March 2016.

[4] Ahmed M. Atallah and El Sayed F. El Tantawy," Direct torque control of machine side multilevel converter for variable speed wind turbines", Science Direct, Elsevier Renewable Energy, VOL 90, PP 1091-1099, 14 July 2015.

[5] Xibo Yuan," A Set of Multilevel Modular Medium-Voltage High Power Converters for 10-MW Wind Turbines," IEEE Transactions on Sustainable Energy, Vol.5, NO. 2, PP. 524 – 534, April 2014.

[6] Md. Rabiul Islam, Youguang Guo, and Jianguo Zhu," A review of offshore wind turbine nacelle: Technical challenges, and research and developmental trends", Science Direct, Elsevier Renewable and Sustainable Energy Reviews, VOL 33, PP 161-176, 31 January 2014.

[7] M. Seixas , R. Melício, V. M. F. Mendes and J. Figueiredo," Three-Level Converter in Offshore Wind Energy Systems: New Strategy for Unbalancing in Capacitors Voltage", Science Direct, Elsevier Procedia Technology, VOL 17, PP 452-460, 2013.

[8] Athanasios Mesemanolis, Christos Mademlis and Iordanis Kioskeridis, "Optimal Efficiency Control

Strategy in Wind Energy Conversion System with Induction Generator", IEEE Journal of Emerging And Selected Topics In Power Electronics, VOL. 1, 2013.
[9] Ming Cheng and Ying Zhu," The state of the art of wind energy conversion systems and technologies: A review", Science Direct, Elsevier Energy Conversion and Management, VOL 88, PP 332-347, 15 August 2014.
[10] R. Kot , M. RolakandM. Malinowski," Comparison of maximum peak power tracking algorithms for a small wind turbine", Science Direct, Elsevier Mathematics and Computers in Simulation, VOL 91, PP 29-40, 7 March 2013.
[11] Dipesh Kumar and Kalyan Chatterjee," A review of conventional and advanced MPPT algorithms for wind energy systems", Science Direct, Elsevier Renewable and Sustainable Energy Reviews, VOL 55, PP 957-970, 9 November 2015.
[12] Ali M. Eltamaly, Hassan M. Farh," Maximum power extraction from wind energy system based on fuzzy logic control", Science Direct, Elsevier Electric Power Systems Research, VOL 97, PP 144–150, 7 January 2013.
[13] Swagat Pati1, Swati Samantray and Nimai Charan Patel," A Novel Adaptive Fuzzy Controller for Performance Improvement of Direct Torque Controlled Induction Generator Employed for Wind Power Applications," IEEE (ICMiCR) conf, Kanjirapally, pp.1-6, 4-6 June 2013.
[14] Swagat Pati1, Swati Samantray and AmiyakumarNaik," Fuzzy Controller Based DTC Scheme for Control of Cage Induction Generator used for Wind Power Application," IEEE (ICCPCT) conf, Nagercoil, pp. 548 - 553, 20-21 March 2014.
[15] D.V.N. Ananth," Enhancement in the Operation of Wind Turbine Based Induction Generator by using Fuzzy Logic Based Direct Torque Control, " IEEE(ICETEEEM), Conf Chennai, pp 159 – 165, 13-15 Dec. 2012
[16] RadiaAbdelli, Djamila Rekioua, Toufik Rekioua , Abdelmounaïm Tounzi ," Improved direct torque control of an induction generator used in a wind conversion system connected to the grid", Science Direct, Elsevier ISA Transactions, VOL 52, PP 525–538,1 July 2013.
[17] Adel Mehdia ,Houssam Medoucea, Salah Eddine Rezguia, Abdelmalek Boulahiaa, Fateh Mehazzem And Hocine Benallaa," PWM Converters and Its Application To The Wind-Energy Generation," Science Direct, Elsevier Energy , PP 523–529 VoL 42, 2013.
[18] J.G. Cardoso , I.R.S. Casella , A.J. Sguarezi Filho , F.F. Costa and C.E. Capovilla " SCIG wind turbine wireless controlled using morphological filtering for power quality enhancement," Science Direct, Elsevier Renewable Energy, PP 303-311, VoL 92, 5 February 2016.
[19] H. MerabetBoulouiha , A. Allali , M. Laouer , A. Tahri , M. Denaï and A. Draou" Direct torque control of multilevel SVPWM inverter in variable speed SCIG-based wind energy conversion system" Science Direct, Elsevier Renewable Energy, VOL 80, PP 140–152, 28 January 2015.
[20] BhavnaJain n, ShailendraJain,R.K.Nema" Control strategies of grid interfaced wind energy conversion system: An overview" Science Direct, Elsevier Renewable and Sustainable Energy Reviews, VOL 47, PP 983–996, 1 April 2015.
[21] YerraSreeniv Vasa Rao and A. Jaya Laxmi" Comparison of the Performance of DTC of Induction Gen Nerator in Wind Energy Conversion System with PI and Neurral Controllers" Science Direct, Elsevier AASRI Procedia, VOL 2, PP 275–281, 2012.
[22] Boris Dumnic, Bane Popadic, DraganMilicevic, Vladimir Katic and DjuraOros "Artificial Intelligence Based Vector Control of Induction Generator without Speed Sensor for Use in Wind Energy Conversion System " International Journal Of Renewable Energy Research, VOL 5, No.1, 2015.
[23] Wang Han, ZhangJianwen and CaiXu," Experiment Study of Squirrel-Cage Induction Generator for the Full-Scale Wind Power Converter" IEEE Conf, Harbin, PP 1457 – 1463, 2-5 June 2012.
[24] Quang-Tho Tran , Anh Viet Truong and Phuong Minh Le " Reduction of harmonics in grid-connected inverters using variable switching frequency" Science Direct, Elsevier Electrical Power and Energy Systems, VOL 82, PP 242–261, 17 March 2016.
[25] HengNian and Yipeng Song" Direct Power Control of Doubly Fed Induction Generator under Distorted Grid Voltage" IEEE Transactions on Power Electronics, VOL. 29, NO. 2,PP 894 – 905, February 2014.
[26] Maurizio Cirrincione, Marcello Pucci and Gianpaolo Vitale" Direct power control of three-phase VSIs for the minimization of common-mode emissions in distributed generation systems" Science Direct, Elsevier Electric Power Systems Research, VOL 81, PP 830–839, 2011.
[27] Nasser Mendoza, JhonPardo, Mar´ıa Mantilla and Johann Petit" A Comparative Analysis of Direct Power Control Algorithms for Three-Phase Power Inverters" IEEE (PES) conf, Vancouver, BC, PP. 1-5, 21-25 July 2013.
[28] G. Brando, A. Dannier, A. Del Pizzo, L.P. Di Noia and I. Spina," Quick and high performance direct power control for multilevel voltage source rectifiers', Science Direct, Elsevier Electric Power Systems Research, VOL 121, PP 15–169, 5 December 2014.
[29] E.G. Shehata" Quick Sliding mode direct power control of RSC for DFIGs driven by variable speed wind turbines', Science Direct, Elsevier Alexandria Engineering Journal, VOL 54, PP 1067–1079, 6 June 2015.
[30] Xie Lei, Xie Da and Zhang Yanchi" Three-level Inverter based on Direct Power Control connecting offshore wind farm", IEEE International Conference on Sustainable Power Generation and Supply, Nanjing, , PP 1- 6, 6 June 2009.
[31] Zhanfeng Song and Changliang Xia" Predictive Direct Power Control for Three-Phase Grid-Connected Converters without Sector Information and Voltage Vector Selection" IEEE Transactions on Power Electronics, VOL. 29, NO. 10, October 2014.
[32] Lei Wang, Shan Zuo, Y. D. Song, and Zheng Zhou3," Variable Torque Control of Offshore Wind Turbine on Spar Floating Platform Using Advanced RBF Neural Network," Hindawi Publishing Corporation, 2014.